Two-step curve fitting combined with a two-layered tissue model to quantify intrinsic fluorescence of cervical mucosal tissue in vivo

Lin, Guo-Sheng, Mok, Chong Ian, Sung, Kung-Bin

Guo-Sheng Lin, Chong Ian Mok, Kung-Bin Sung, "Two-step curve fitting combined with a two-layered tissue model to quantify intrinsic fluorescence of cervical mucosal tissue in vivo
," Proc. SPIE 11925, Biomedical Imaging and Sensing Conference 2021, 1192513 (27 October 2021); doi: 10.1117/12.2615715

SPIE.

Event: SPIE Technologies and Applications of Structured Light, 2021, Online, Japan

Two-Step Curve Fitting Combined with a Two-Layered Tissue Model to Quantify Intrinsic Fluorescence of Cervical Mucosal Tissue in Vivo

Guo-Sheng Lin[a], Chong Ian Mok[a], Kung-Bin Sung[abc]

[a]Graduate Institute of Biomedical Electronics and Bioinformatics, National Taiwan University, No. 1, Sec. 4, Roosevelt Rd., Taipei, Taiwan (R.O.C.)

[b]National Taiwan University, Department of Electrical Engineering, No. 1, Sec. 4, Roosevelt Rd., Taipei, Taiwan (R.O.C.)

[c]National Taiwan University, Molecular Imaging Center, No. 1, Sec. 4, Roosevelt Rd., Taipei, Taiwan (R.O.C.)

Abstract

Fluorescence spectroscopy (FS) has been used to characterize tissue fluorophores in vivo for the diagnosis of precancers in the uterine cervix. In this study, a two-step curve fitting process is established to extract the intrinsic fluorescence intensity and spectrum of fluorophores including NADH and FAD in the epithelium and collagen crosslinks in the stroma. Forward Monte Carlo (MC) models of diffuse reflectance spectroscopy (DRS) and FS are replaced by artificial neuron networks to improve the computation speed. First, absorption and scattering coefficients of the two tissue layers and the epithelial thickness are estimated from DRS data. Second, the genetic algorithm is used to find the best set of intrinsic fluorescence parameters of the three fluorophores that best fit measured FS data. Results suggest that the two-layered tissue model outperforms conventional homogeneous tissue models in extracted tissue optical properties. Intrinsic fluorescence parameters are extracted from in-vivo spectra measured on 31 subjects.

Keywords: diffuse reflection spectroscopy, fluorescence spectroscopy, Monte Carlo method, artificial neuron network, genetic algorithm

I Introduction

Main fluorescent substances, also known as fluorophores, in mucosal tissue include nicotinamide adenine dinucleotide (NADH), flavin adenine dinucleotide (FAD) and collagen cross-links. The NADH concentration in a cell is associated with the regulation of ATP and DNA repair ability of the cell.[1] Therefore, using optical methods to quickly obtain the content of NADH in tissues has been proposed as an indicator of the effectiveness of cancer treatment for the development of anti-cancer drugs, replacing smear examinations to reduce examination costs.

According to the research of R. Drezek et al., cervical cells in suspension and collagen gel phantoms were used to measure the absorption spectrum and emission spectrum at each wavelength to obtain contributions of NADH and collagen cross-links to fluorescence spectra measured in vivo. However, the physical differences of the subjects may

Biomedical Imaging and Sensing Conference 2021, edited by Toyohiko Yatagai, Yoshihisa Aizu, Osamu Matoba, Yasuhiro Awatsuji, Yuan Luo, Proc. of SPIE Vol. 11925, 1192513 · © 2021 SPIE · 0277-786X · doi: 10.1117/12.2615715

affect the shape and intensity of fluorescence spectra. In addition, the fluorescence response of cells in an in vitro environment is also different from that in an in vivo environment, causing errors in the results.[2] Therefore, this research uses two-step curve fitting based on forward DRS and FS models implemented by artificial neural networks (ANNs) and the genetic algorithm to solve the shape and intensity contributions of the main fluorophores in cervical mucosa in vivo.

II clinical experiments and curve fitting progress

1. Diffuse Reflection and Fluorescence Spectroscopy

The optical system used in this article measures DRS and FS in the visible wavelength range via multiple optical fibers.[3] Three source-detector separations (SDS) are used as a set, and there are two sets including 0.22, 0.41, 0.61 mm and 0.215, 0.45, 0.73 mm respectively. The non-uniform spectral response of the optical system is linearly corrected by phantoms with known scattering and absorption coefficients.[4, 5] Finally, in-vivo spectra are obtained from 31 subjects, nine of which contain both precancerous and normal cervical tissues, and the rest only normal cervical tissue.

2. Monte Carlo method and two-layered tissue model

The Monte Carlo method is applied to model the random walk of photons in biological tissues by considering tissue scattering, absorption, reflection and refraction events. Diffuse reflectance and fluorescence emission photons that reach the detection fibers at incidence angles within the fiber acceptance angle are recorded for each wavelength in 408-750 nm range with a 3 nm increment.[6-8]

A two-layered tissue model is used to simulate the cervical tissue. The two layers are assumed to be parallel and homogenous. The upper-layer represents the epithelium which contains NADH and FAD, and the lower-layer represents the stroma and contains blood, and collagen. Nine parameters including A_{up}, K_{up}, A_{bt}, k_{bt}, tissue oxygen saturation (StO_2), hemoglobin concentration (C_{Hb}), scale factor of the upper layer absorption coefficient (α), volume fraction of collagen (C_{coll}), and the upper layer thickness (th) are used to calculate the absorption coefficient and scattering coefficient of the upper- and lower-layers.

$$\mu_{a_{up}}(\lambda) = \alpha \times \mu_{a_{epi}}(\lambda) \tag{1}$$

$$\mu_{a_{bt}}(\lambda) = C_{Hb}\left(\frac{\ln(10)}{64532} \times StO_2 \times \mu_{a_{oxy}}(\lambda) + \frac{\ln(10)}{64500} \times (1 - StO2) \times \mu_{a_{deox}}(\lambda)\right) + C_{coll} \times \mu_{a_{coll}}(\lambda) \tag{2}$$

$$\mu_{s_{(up\ or\ bt)}}(\lambda) = A_{(up\ or\ bt)} \times \frac{\lambda^{-k_{(up\ or\ bt)}}}{1-g_{(up\ or\ bt)}} \tag{3}$$

$\mu_{a_{epi}}$ is the absorption coefficient of epithelial cells[9], $\mu_{a_{oxy}}$ and $\mu_{a_{deox}}$ are the molar extinction coefficient of oxygenated and deoxygenated blood, respectively, $\mu_{a_{coll}}$ is the absorption coefficient of 100% collagen, and g is the anisotropic factor.[10-12]

3. Artificial Neural Network (ANN)

ANNs are trained to replace the forward Monte Carlo models to calculate the detected diffuse reflectance and fluorescence emission mentioned in Section II.2 for each SDS.[13] The ANNs for DRS require five input parameters, namely the upper- and lower-layer absorption coefficients ($\mu_{a_{up}}$, $\mu_{a_{bt}}$), the upper- and lower-layer scattering coefficients ($\mu_{s_{up}}$, $\mu_{s_{bt}}$), and the upper layer thickness . For the FS ANNs three more input parameters are needed including $\mu_{a_{bt}}$, $\mu_{s_{up}}$ and $\mu_{s_{bt}}$ at the excitation wavelength of 365 nm. Separate FS ANNs are trained for

fluorescence originating from fluorophores in the upper- and lower-layer, respectively.

The ANN models of DRS and FS use Z-score to normalize the input data and the natural logarithmic function to scale the output light intensity. Finally, we confirm that the test data error of trained DRS/FS ANN is less than the average coefficient of variation of multiple runs of DRS/FS MC simulations (using the same set of input parameters) and less than 2%.

4. two-step curve fitting

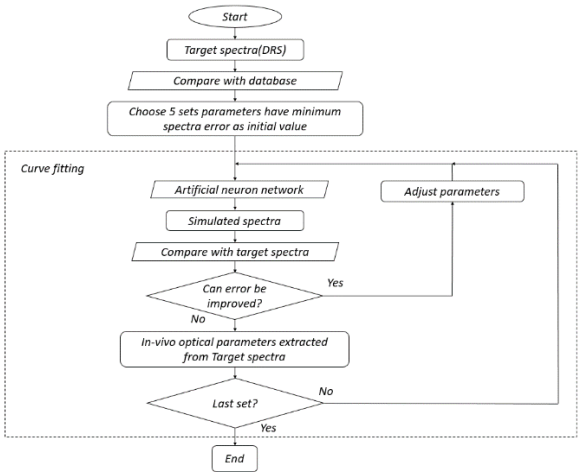

Figure 1. Flow chart of the first curve fitting step (DRS fitting)

Curve fitting is used to minimize the root-mean-square percentage error (RMSPE) between simulated spectra and target spectra. In the first step of curve fitting (Figure 1.), DR spectra measured from the cervical mucosa in vivo are calibrated and compared to spectra in a pre-calculated database to find five sets of initial parameter values with the smallest RMSPE. From each initial set the nine parameters introduced in Section II.2 are updated iteratively to find the parameter combination with the lowest RMSPE as the extracted tissue parameters. In the second step of curve fitting (Figure 2.), the tissue parameters extracted in the first step are used to calculate the upper- and lower-layer fluorescence spectra by the trained FS ANNs. The fluorescence emission spectral shape of each fluorophore is modeled by a skew-normal distribution with its mean, standard deviation, and skewness as unknown parameters. The intensity of the intrinsic fluorescence of each fluorophore is represented by another parameter called fluorescence efficiency which combines the quantum yield and the absorption coefficient (at the excitation wavelength = 350 nm) of the corresponding fluorophore [14]. The measured fluorescence spectra after calibration are iteratively fitted by searching for the best set of parameters to achieve the least RMSPE using the genetic algorithm.

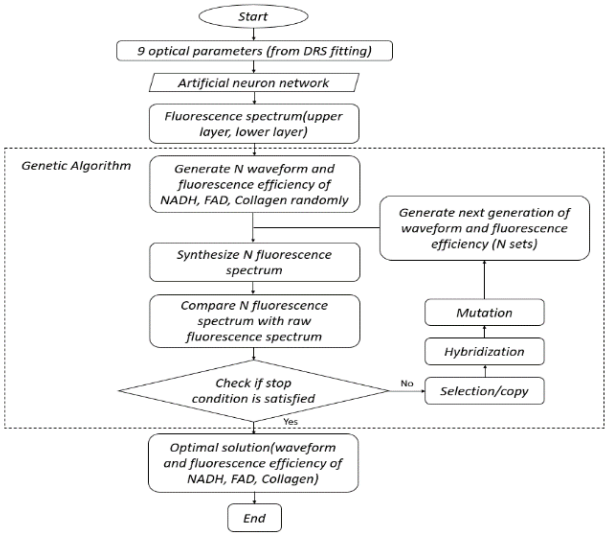

Figure 2. Flow chart of the second curve fitting step

III Results and Discussion

In one of the 31 sets of clinical spectra, the average of 3 SDSs RMSPE of the one-layer curve fitting model is about 40% (Figure 3. top blue circle) and the two-layered curve fitting model is about 4% (Figure 3. top red circle). In another clinical spectrum, the diffuse reflectance spectrum error between the fitting result and the clinical spectrum is

about 8% and the error between the clinical fluorescence spectrum and the fitting result is about 19 %. (Figure 3. bottom)

In the DRS curve fitting, the one-layer model has a large error. It is necessary to further adjust the upper and lower bounds of the parameters and the step size during fitting. However, the two-layered model can obtain significantly better fitting results than the one-layer model because the multi-layer model is more similar to the actual structure of tissue. At the shortest SDS and at the wavelength of 400-450 nm, the absorption of red blood cells has a large error. In FS, the wavelength 400-420 nm is not consistent with the clinical spectrum. It is presumed to be the absorption of red blood cells in the lower spectrum. Due to the low complexity of the skew distribution, the final spectrum is relatively smooth. As a result, some irregular shapes on the clinical spectrum are difficult to fit accurately.

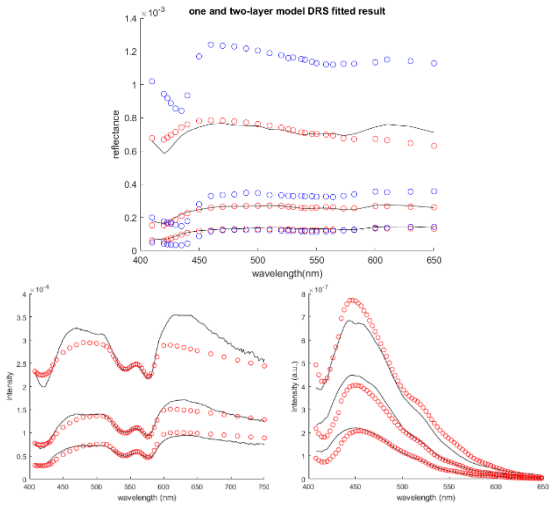

Figure 3. Clinical DRS (Top and bottom left) and FS (bottom right) curve fitting results using one-layer (blue circles) and two-layered (red circles) models. The three lines from top to bottom in each panel are spectra at an SDS of 0.22, 0.41 and 0.61 mm, respectively.

The fitting result may be affected by the optical parameters of diffuse reflectance fitting. If the spectral error of the fitting of diffuse reflectance spectrum is too high, it may affect the result of fluorescence fitting. After more clinical fluorescence spectra become available in the future, we may try to adjust the range of parameters and the mathematical models of absorption and scattering coefficients.

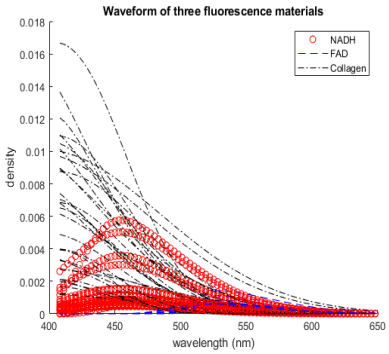

Figure 4. Intrinsic fluorescence spectra of the three fluorophores extracted from 31 sets of clinical fluorescence spectra

Through the two-step fitting process, including curve fitting and genetic algorithm, we analyzed the optical parameters of the tissue using DRS and quantified the intrinsic fluorescence of cervical mucosa tissue (Figure. 4), including NADH (10%), FAD (6%) and Collagen (84%) which are consistent with previous studies.[2] It is also proved through the test spectrum that when the fluorescence yield is within a certain range, the proposed two-step curve fitting method can be used to separate contributions of the three fluorophores to the detected fluorescence spectrum. In addition, a neural network is used to replace the Monte Carlo method to generate simulated spectra, thereby improving the efficiency of curve fitting, so that the model can obtain quantitative data more quickly.

References

[1] Pelzmann, B. et al., "NADH supplementation decreases pinacidil-primed I K ATP in ventricular cardiomyocytes by increasing intracellular ATP," *Br J Pharmacol 139*(4), 749-754 (2003).

[2] Drezek, R. et al., "Understanding the contributions of NADH and collagen to cervical tissue fluorescence spectra: modeling, measurements, and implications," *J Biomed Opt 6*(4), 385-396 (2001).

[3] Huang, T. H., "Quantifying In-Vivo Tissue Optical Parameters of Precancerous Cervical Lesions using a Portable Reflectance Spectroscopy System," in *Graduate Institute of Biomedical Electronics and Bioinformatics*, 1-59, National Taiwan University (2017).

[4] Chuang, M.-J., "Construction and Verification of a Portable Diffuse Reflectance Spectroscopy System for Clinical Studies," in *Graduate Institute of Biomedical Electronics and Bioinformatics*, 1-51, National Taiwan University (2015).

[5] Hsiao, Y.-H., "Using Fluorescence Spectroscopy to Distinguish Precancerous Mucosa," in *Graduate Institute of Biomedical Electronics and Bioinformatics*, 1-60, National Taiwan University (2015).

[6] Henyey, L. G., and J. L. Greenstein, "Diffuse radiation in the galaxy," *Annales dAstrophysique* 117 (1940).

[7] Welch, A. et al., "Propagation of fluorescent light," *Lasers in Surgery and Medicine 21*(2), 166-178 (1997).

[8] Pery, E. et al., "Monte Carlo modeling of multilayer phantoms with multiple fluorophores: simulation algorithm and experimental validation," *Journal of Biomedical Optics 14*(2), 024048 (2009).

[9] Farrell, T. J., M. S. Patterson, and B. J. M. p. Wilson, "A diffusion theory model of spatially resolved, steady-state diffuse reflectance for the noninvasive determination of tissue optical properties in vivo," *Medical physics 19*(4), 879-888 (1992).

[10] Qu, J. et al., "Optical properties of normal and carcinomatous bronchial tissue," *Applied Optics 33*(31), 7397-7405 (1994).

[11] Nunez, A. S., "A physical model of human skin and its application for search and rescue," AIR FORCE INST OF TECH WRIGHT-PATTERSON AFB OH SCHOOL OF ENGINEERING (2009).

[12] Bhandari, A. et al., "Modeling optical properties of human skin using Mie theory for particles with different size distributions and refractive indices," *Optics Express 19*(15), 14549-14567 (2011).

[13] Tsui, S.-Y. et al., "Modelling spatially-resolved diffuse reflectance spectra of a multi-layered skin model by artificial neural networks trained with Monte Carlo simulations," *Biomed Opt Express 9*(4), 1531-1544 (2018).